

Solving the octant degeneracy with the Silver channel

Davide Meloni*

*Dip. di Fisica, Università di Roma Tre and INFN, Sez. di Roma Tre,
Via della Vasca Navale 84, I-00146 Roma, Italy*

We study the potential of the combination of the golden ($\nu_e \rightarrow \nu_\mu$) and silver ($\nu_e \rightarrow \nu_\tau$) channels to solve the octant degeneracy affecting the measurement of θ_{13} and δ at future neutrino factories. To search for τ leptons produced in ν_τ charged-current interactions, we consider two different detectors: the Emulsion Cloud Chamber detector (ECC) and the Liquid Argon Time Projection Chamber (LAr TPC). We show that, when using similar detector masses, the upgraded version of the ECC detector (sensitive also to hadronic τ decay modes) and the LAr TPC detector have comparable sensitivities to the octant of θ_{23} , being able to discriminate the two solutions for $\sin^2(2\theta_{13}) \gtrsim 10^{-3}$ at 3σ level if $\theta_{23} = 40^\circ$. We also show that the same setups are able to see deviation from maximal mixing as small as $\sim (4-6)\%$ (at 3σ) if θ_{13} is close to its upper bound.

PACS numbers: 95.85.Ry, 96.40.Tv, 14.60.Pq

I. INTRODUCTION

The simultaneous measurement of the two still unknown neutrino mixing parameters θ_{13} and δ can be considered as one of the main neutrino-physics goal for the next decade [1]. The ideal places where to look for the signal induced by the small (vanishing ?) θ_{13} and the unconstrained phase δ are the appearance channels $\nu_e \rightarrow \nu_\mu$ [2] and $\nu_e \rightarrow \nu_\tau$ [3] (which then deserve the name of "golden" and "silver" channels, respectively) and any other transition obtained from them by symmetry relation like T or CP. The reason for this success is mainly ascribed to the leading θ_{13} dependence of the transition probabilities and the next-to-leading dependence on δ , a characteristic not shared by the disappearance channels. If one uses the parametrization of the three-family leptonic mixing matrix U_{PMNS} [4] suggested in the PDG [5], θ_{13} and δ always appear in the combination $\sin \theta_{13} e^{\pm i\delta}$ and a measurement of the CP-phase δ cannot be achieved independently on θ_{13} : the two parameters have to be measured at the same time. Such a correlation stains the achievable precision on the parameter measurements since some θ_{13} and δ can reproduce the same "true" physics (number of expected events) at some confidence level, a situation which is known as the *degeneracy problem*. The (θ_{13}, δ) -pairs which mimic the value chosen by Nature are called *clone points* and come from our ignorance about the "true" θ_{13} and δ (intrinsic clone), the sign of the atmospheric mass difference (sign clones) and the octant to which θ_{23} belongs, if not maximal (octant clones) [6]-[10]. Many papers have already discussed the problem of the *eightfold* degeneracy and its possible solutions, the common denominator being the need to combine as many independent informations as possible (spectral informations, different L/E setups, different transition channels...) with the aim of locating the clone points in different region of the (θ_{13}, δ) parameter space: in this way, the statistical significance of the fake solutions decreases and one can hope to solve the degeneracies [11].

In this paper we want to point out the importance of using the silver transition (in combination to the golden one) to solve the octant degeneracy at the neutrino factories [12]. In the next section, we briefly revise some theoretical aspects related to the location of the fake octant solutions in the (θ_{13}, δ) -plane and the promising synergy between the golden and silver channels; in Sect. III, we discuss the potential of an Emulsion Cloud Chamber detector (ECC) to help in solving the octant degeneracy and we discuss the better performance of an improved version of it, which allows to look for the hadronic τ decays, also (the *silver** option, [13]); Sect. IV is devoted to the study of the octant degeneracy using the Argon Time Projection Chamber (LAr TPC) whereas in Sect. V we briefly describe the possibility to establish deviation from maximal mixing. In Sect. VI we eventually draw our conclusions.

*Electronic address: meloni@fis.uniroma3.it

II. THE OCTANT DEGENERACY

The octant degeneracy originates because neutrino experiments are looking for ν_μ, ν_e disappearance or $\nu_\mu \rightarrow \nu_\tau$ oscillations, where θ_{23} appears only through $\sin^2 2\theta_{23}$. However, even if the dominant term in the $\nu_\mu \rightarrow \nu_\mu$ transition probability is completely symmetric under $\theta_{23} \rightarrow \pi/2 - \theta_{23}$, subleading effects could in principle break this symmetry (although very difficult to isolate, the combination of appearance and disappearance channels at a neutrino factory with $L=7000$ Km can do the job for relatively large θ_{13} , [14]) and help in the octant discrimination (see, e.g., [15]-[18]). At the probability level, the octant degeneracy manifests itself in the $\nu_\alpha \rightarrow \nu_\beta$ transition ($\alpha \neq \beta$) when the system of equations

$$P_{\alpha\beta}^\pm(\bar{\theta}_{13}, \bar{\delta}, \bar{\theta}_{23}) = P_{\alpha\beta}^\pm(\theta_{13}, \delta, \pi/2 - \theta_{23}) \quad (2.1)$$

admits solutions for θ_{13} and δ different from the values chosen by Nature (and indicated with a bar). Here, $P_{\alpha\beta}^\pm$ are the transition probabilities for neutrinos and antineutrinos, respectively. The equations can be numerically solved in the exact form; however, to get some light on the analytical behavior of the clone solutions, we expand the probabilities $P_{\alpha\beta}^\pm$ in vacuum for small θ_{13} , $\Delta_\odot/\Delta_{atm}$ and $\Delta_\odot L$ [2]. We then obtain:

$$\begin{cases} P_{e\mu}^\pm(\bar{\theta}_{13}, \bar{\delta}) = X_\mu \sin^2(2\bar{\theta}_{13}) + Y \cos(\bar{\theta}_{13}) \sin(2\bar{\theta}_{13}) \cos(\pm\bar{\delta} - \frac{\Delta_{atm}L}{2}) + Z_\mu \\ P_{e\tau}^\pm(\bar{\theta}_{13}, \bar{\delta}) = X_\tau \sin^2(2\bar{\theta}_{13}) - Y \cos(\bar{\theta}_{13}) \sin(2\bar{\theta}_{13}) \cos(\pm\bar{\delta} - \frac{\Delta_{atm}L}{2}) + Z_\tau \end{cases} \quad (2.2)$$

and

$$\begin{cases} X_\mu = \sin^2(\theta_{23}) \sin^2\left(\frac{\Delta_{atm}L}{2}\right); & X_\tau = \cos^2(\theta_{23}) \sin^2\left(\frac{\Delta_{atm}L}{2}\right); \\ Y = \sin(2\theta_{12}) \sin(2\theta_{23}) \left(\frac{\Delta_\odot L}{2}\right) \sin\left(\frac{\Delta_{atm}L}{2}\right); \\ Z_\mu = \cos^2(\theta_{23}) \sin^2(2\theta_{12}) \left(\frac{\Delta_\odot L}{2}\right)^2; & Z_\tau = \sin^2(\theta_{23}) \sin^2(2\theta_{12}) \left(\frac{\Delta_\odot L}{2}\right)^2. \end{cases} \quad (2.3)$$

with $\Delta_{atm} = \Delta m_{atm}^2/2E_\nu$ and $\Delta_\odot = \Delta m_\odot^2/2E_\nu$. The three terms in eq. (2.2) are called the *atmospheric*, *interference* and *solar* terms, respectively [19]. Two comments are in order. The different sign in front of the interference term among the golden and silver transitions has been recognized as very useful to solve the intrinsic degeneracy for $\theta_{13} \gtrsim \mathcal{O}(1^\circ)$ [3, 20] (below that value the statistics of silver events being too small to be significant). The second important point is the different dependence on θ_{23} in X_μ, X_τ and Z_μ, Z_τ since $X_\tau = X_\mu(\theta_{23} \rightarrow \pi/2 - \theta_{23})$ and $Z_\tau = Z_\mu(\theta_{23} \rightarrow \pi/2 - \theta_{23})$, which is precisely the reason why we can profit of the silver channel to solve the octant degeneracy. In order to find simple analytical solutions of eq. (2.1), we introduce the small parameter ε , which represents the deviation of θ_{23} from maximal mixing, $\varepsilon = \theta_{23} - \pi/4$; then, a value $\varepsilon < 0$ ($\varepsilon > 0$) means that θ_{23} is in the first (second) octant. Since it will be important for later applications, we remind that, in the atmospheric regime ($X_{\mu,\tau} \gg Z_{\mu,\tau}$) and small ε , the intrinsic clones are located in the fake points [11, 19]:

$$\begin{cases} \delta_{\text{int}} & \sim \pi - \bar{\delta} \\ (\sin^2 2\theta_{13})_{\text{int}} & \sim \sin^2 2\bar{\theta}_{13} \pm 4 \cos \bar{\delta} \sin 2\theta_{12} \left(\frac{\Delta_\odot L}{2}\right) \cot\left(\frac{\Delta_{atm}L}{2}\right) + \mathcal{O}(\varepsilon) \end{cases} \quad (2.4)$$

where the positive (negative) sign refers to the golden (silver) channel. We recover the known result that the shift in θ_{13} is opposite for the two transitions whereas the location in δ is quite independent on θ_{13} .

Let us now go back to eq. (2.1). We expect two different solutions: one of them is a mirror of the true point (*S1*) whereas the other one is a mirror of the intrinsic clone in eq. (2.4) (*S2*). Working in the atmospheric regime (the one in which the silver statistics is not too small compared to the golden one), and up to the first order in ε (i.e., neglecting $\mathcal{O}(\varepsilon \cdot \Delta_\odot L)$ terms), we find:

$$S1: \quad \begin{cases} \sin \delta & \propto (1 \mp 2\varepsilon) \sin \bar{\delta} \\ \sin^2 2\theta_{13} & \propto (1 \pm 4\varepsilon) \sin^2 2\bar{\theta}_{13} \end{cases} \quad (2.5)$$

$$S2 : \begin{cases} \sin \delta & \propto (\sin \delta)_{\text{int}} \mp 2\varepsilon \sin \bar{\delta} \\ \sin^2 2\theta_{13} & \propto (\sin^2 2\bar{\theta}_{13})_{\text{int}} \pm 4\varepsilon \sin^2 2\bar{\theta}_{13} \end{cases} \quad (2.6)$$

where the upper (lower) sign refers to the golden (silver) channel and the subscripts *int* refer to the solution of eq. (2.4).

It is quite interesting to observe that in *S1* the location of the clones always goes in opposite direction for golden and silver transitions, which means that the shifts $\theta_{13} - \bar{\theta}_{13}$ and $\delta - \bar{\delta}$ have different sign. Moreover, the distance between clones increases for larger deviations from maximal mixing. Notice that, in the limit $\varepsilon \rightarrow 0$, *S1* reduces to the input point, which means that this solution is quite independent on L/E and, then, much more difficult to eliminate with methods based on energy resolution or different baselines.

The solution *S2* shows the interesting behavior that the octant clones are close to the intrinsic degeneracy; then, if the silver channel is useful to solve the intrinsic degeneracy, it could also be able to eliminate/reduce the impact of the octant degeneracy. Also in this case we can observe an opposite sign in front of the ε term, which slightly increases (reduces) the distance in θ_{13} between the golden and silver clones for $\varepsilon > 0$ ($\varepsilon < 0$).

As a final remark, notice that the position in δ is *always* very close to the value of $\bar{\delta}$ (for *S1*) or δ_{int} (for *S2*) since a shift of the sinus function proportional to ε translates in a much smaller deviation of the argument of the same function.

The previous considerations, obtained from very simple analytical formulae in vacuum, describe quite well the general position of the octant clone points, even including matter effects, whose impact is negligible for *S1* (due to the mild dependence on L/E) and more evident for *S2* (but not so large to modify our conclusions, as we have carefully verified with numerical simulations). More important, we can repeat the whole calculation using the number of expected events at a given neutrino facility (instead of probabilities) and solving the analogous system of equations for rates in the exact form. In this way, the location of the clones will be much more similar to the experimental expectation since we fold the probabilities with fluxes and cross sections [11]. To be specific, we illustrate this point using two detectors able to measure the golden and silver transitions at the same baseline, $L = 4000 \text{ Km}^1$. Other experimental details like absolute flux normalization, detector mass and overall efficiencies are unimportant since they cancel when evaluating the integrated eq.(2.1). The results obtained with this detector configuration and for $\bar{\delta} = 54^\circ$ and $\varepsilon = -2^\circ$ are shown in Fig. (1).

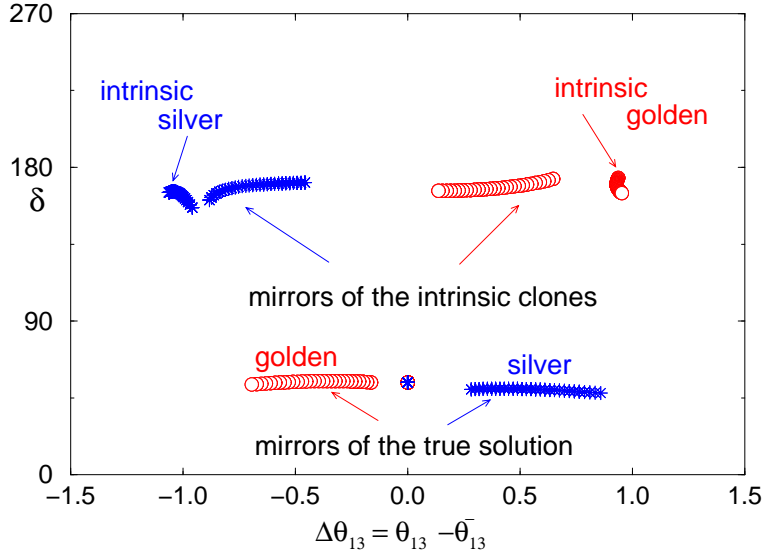


FIG. 1: *Intrinsic and octant clone locations in the $(\Delta\theta_{13}, \delta)$ -plane. See text for details.*

The points represent the location of the intrinsic and octant clones, for the golden and silver channels. For a fixed $\bar{\theta}_{13}$, we calculate the fake θ_{13} and δ and put them in the $(\Delta\theta_{13} = \theta_{13} - \bar{\theta}_{13}, \delta)$ -plane. Varying the input $\bar{\theta}_{13}$, we are

¹ In [13], it has been shown that to maximize the statistical significance of the silver channel the best choice, and also the most economic one, is to place the golden and silver detectors at the same baseline.

able to build the *clone flow* for a given $\bar{\delta}$ [11]. All the features previously described can be clearly seen: the golden and silver intrinsic clones are located in opposite directions ($\Delta\theta_{13} > 0$ or $\Delta\theta_{13} < 0$), the mirrors of the intrinsic clones follow them (and are much less separated than the intrinsic solutions thanks to the $\mathcal{O}(\varepsilon)$ terms in eq. (2.6)) whereas the δ solutions of eq. (2.5) show, as expected, a scarce dependence on $\bar{\theta}_{13}$ and are very close to both the input values and δ_{int} . From the theoretical point of view, all the clones are far away to each other and one can hope to solve the degeneracy.

III. COMBINING THE MIND AND ECC DETECTORS

In order to verify how realistic these conclusions are, we perform a simulation of a neutrino factory in the spirit of [2], taking $1 \cdot 10^{21} \mu^+ \times 4$ years, $1 \cdot 10^{21} \mu^- \times 4$ years [1] and putting the detectors at the same baseline $L = 4000$ Km². To look for golden muons, we use an improved version of the MIND detector described in [22]: in particular, we divide the signal and the background in 10 energy bins of variable size [23], according to the energy resolution considered in [24]. We also estimate efficiency and background from [24]. To search for τ events we use the ECC detector, with efficiencies and backgrounds from [20] and divide the signal in 5 energy bins. The mass of the detector is 5 Kton. We also considered a conservative 10% of systematic error for the silver detector and a 2% for the golden one.

The χ^2 analysis, along the lines described in [3], is performed simulating four input points, namely $(\sin^2 2\bar{\theta}_{13}, \bar{\delta}) = (1.2 \cdot 10^{-3}, 300^\circ)$, $(2.7 \cdot 10^{-3}, 150^\circ)$, $(4.9 \cdot 10^{-3}, 0)$ and $(7.6 \cdot 10^{-3}, 90^\circ)$. The other oscillation parameters are fixed to the best fit values quoted in [25], except for θ_{23} , which we take away from maximal mixing, namely $\theta_{23} = 43^\circ$ ($\varepsilon = -2^\circ$). We used the GLoBES software [26] to compute the expected rates at the neutrino factory.

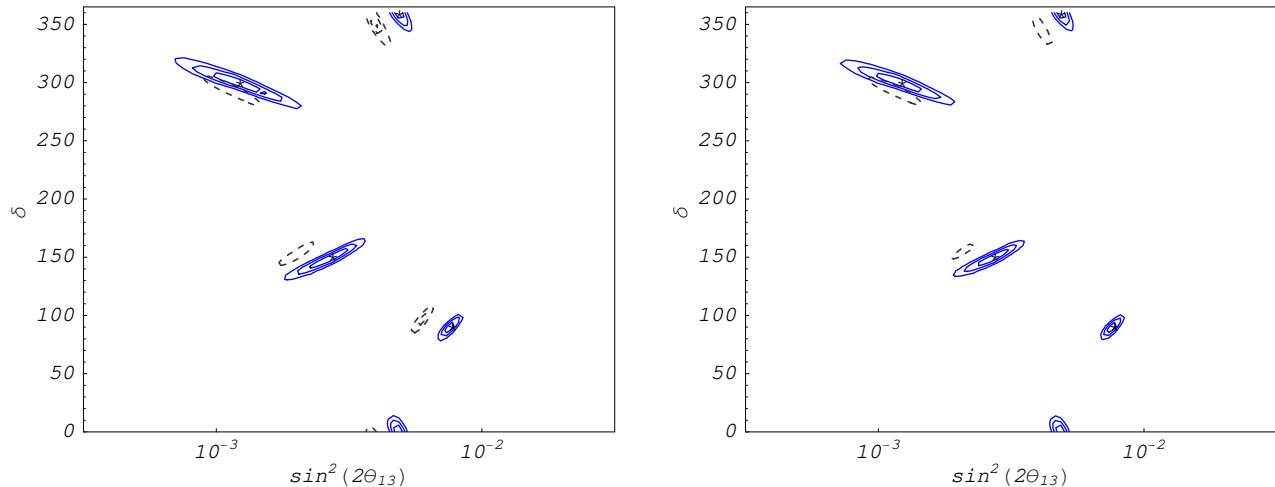


FIG. 2: 1, 2 and 3 σ CL contours for the simulated points $(\sin^2 2\bar{\theta}_{13}, \bar{\delta}) = (1.2 \cdot 10^{-3}, 300^\circ)$, $(2.7 \cdot 10^{-3}, 150^\circ)$, $(4.9 \cdot 10^{-3}, 0)$, $(7.6 \cdot 10^{-3}, 90^\circ)$ in the $(\sin^2 2\theta_{13}, \delta)$ -plane. Continuum lines refer to the true and intrinsic points, dashed lines to the octant clones. Left panel: results obtained combining the events from MIND and ECC detectors. Right panel: results obtained using the combination MIND+ECC* detectors.

The impact of using the silver channel in solving the octant degeneracy (the intrinsic one being already solved for the representative points used in this analysis) can be seen in the left panel of Fig. (2), in which we show the 1, 2 and 3 σ CL obtained combining the golden and silver events. As it can be seen, the impact of the octant clones (dashed lines) in the measurement of θ_{13} and δ can be relevant; for any of the input points taken into account, the octant mirrors of the true points reduce the achievable precision in the measurement of the unknowns, especially for θ_{13} ; moreover, according to our comments below eqs. (2.5-2.6), the golden octant clones reside on the left of the input points whereas the value of the fake δ is closed to that of the input and intrinsic points.

We have checked that very similar results can be obtained if we use the golden events only, mostly due to the quite good performance of the improved MIND detector and the relatively small statistics at the ECC detector. It is clear

² Notice that the total number of stored muons, $8 \cdot 10^{21}$, is in agreement with the experimentally feasible $5 \cdot 10^{20}$ muons per year and per baseline, adopted in the case of a neutrino factory pointing toward two detectors located at two different baselines [21].

that an improvement of the silver detector is needed to take full advantage of the theoretical synergy with the golden channel expressed in eqs. (2.5-2.6).

With the aim of improving the physics performance of the silver channel, some detector features have been already discussed even though, at least to our knowledge, the results of a full simulation of the new version of the detector has not been published yet (see [1]). Some new features rely on the possibility to perform a dE/dx measurement to reduce the charm background and to scan more than one brick per event, which would increase the signal detection efficiency by about 20% [27]. Most notably, the possibility to search for the hadronic τ decay modes has been also discussed; it would allow a branching ratio gain ($\tau \rightarrow h$ and $\tau \rightarrow e$ channels) and a further reduction of the background from hadronic interactions. This can be achieved embedding the ECC detector in a magnetic field and adding a Total Active Scintillator Detector after the ECC in such a way to better discriminate between electrons and pions [27]³. These considerations inspired the authors of [13] to introduce the so-called *silver** (that, to avoid confusion with detectors, in the following will be called ECC*). They assume that the detector improvements allow an increase of the silver statistics by a factor of five and, thanks to the improvements necessary for identifying hadronic tau decays, the background is only a factor of three its standard value. In the following we will assume the ECC* setup but we maintain the same detector mass used before. With such a setup, the capability of the silver transition to solve the octant degeneracy is improved, as we can see in the right panel of Fig. (2), in which we plot the same contours as in the left panel but using the ECC* setup. For the larger $\sin^2 2\bar{\theta}_{13} = 7.6 \cdot 10^{-3}$, the clone point disappears whereas for the other values of $\sin^2 2\bar{\theta}_{13}$ the clones only appear at 3σ confidence level.

In order to generalize our results, we compute the sensitivity to the θ_{23} -octant: for any value of δ , we look for the smaller value of θ_{13} for which no degenerate octant solutions appear at 3σ CL. The results are shown in Fig. (3).

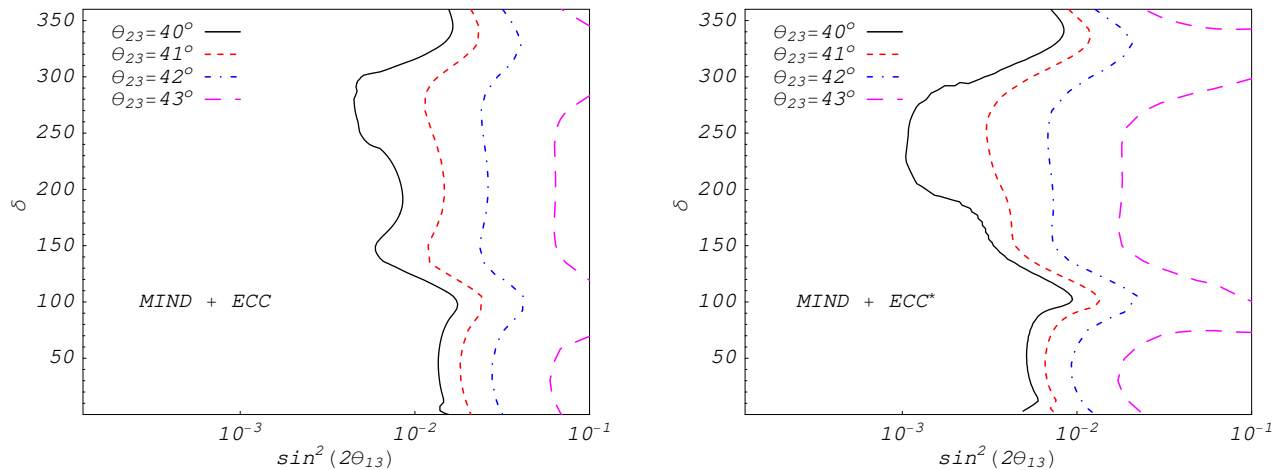


FIG. 3: Sensitivity to the θ_{23} octant at 3σ CL. The results are obtained combining the MIND+ECC detectors for different θ_{23} , from 40° to 43° . In the left panel the sensitivity has been calculated using the standard ECC whereas in the right panel the ECC* has been employed.

In the left panel, we compute the sensitivity for the combination of MIND+standard ECC. These results are simply explained with the help of eqs. (2.5-2.6) since the distance between golden and silver octant clones is increased for larger deviation from maximal mixing (that is, larger $|\varepsilon|$); thus, a much better performance is reached for $\theta_{23} = 40^\circ$. The improvement reached using the ECC* detector is clearly seen in the right panel; for each value of θ_{23} , a better performance by a factor of 2 – 3 can be seen, depending on the value of the CP phase considered. In particular, in the range $\delta \in [200^\circ, 300^\circ]$, the sensitivity exhibits a sort of plateau around $\sin^2(2\theta_{13}) \sim 1.04 \cdot 10^{-3}$ for $\theta_{23} = 40^\circ$ and $\sin^2(2\theta_{13}) \sim 1.80 \cdot 10^{-2}$ for $\theta_{23} = 43^\circ$, whereas the minima are around $\delta \sim 100^\circ$. This is due to the fact that for δ close to maximal CP violation, the number of golden events is extremely large and the silver statistics is comparably small in such a way not to be able to help in solving the degeneracy⁴.

³ It would also allow to look for the platinum transition $\nu_\mu \rightarrow \nu_e$.

⁴ At smaller confidence level, we have observed that the octant degeneracy can be solved also for $\sin^2(2\theta_{13})$ well below 10^{-3} . This has to be certainly ascribed to the action of the solar term Z_μ in the first relation in eq. (2.2), thus the golden channel alone is able to get rid of the degeneracy for smaller θ_{13} , for which the silver statistics can be completely neglected.

IV. THE LIQUID ARGON TIME PROJECTION CHAMBER

The Liquid Argon Time Projection Chamber (LAr TPC) is a detector for uniform and high accuracy imaging of massive active volumes. It is based on the fact that in highly pure Argon, ionization tracks can be drifted over distances of the order of meters [28]. Thanks to its high granularity target and its calorimetric properties, this design provides a clean identification and measurement of all three neutrino flavours, and in particular ν_τ 's, to which we are interested in. Following [29], we assume a non-magnetized target-detector and that charge discrimination is only available for muons reaching and external magnetized-Fe spectrometer. Notice that a very large magnetized LAr TPC with a mass ranging from ~ 10 to 100 Kton has been recently proposed [30]. Our aim here is to estimate, depending on the adopted detector mass, the potential of such a large detector in solving the octant degeneracy. As far as we know, a dedicated simulation of the detector response to the silver channel has not been carried out, at least at the sophisticated level reached in [20]. This means that the estimate of the background affecting the measurement of the silver candidates events should rely to some *reasonable* assumption; we then adopt the aptitude of considering all the background sources already described in [20] and to study the possible detector response to them [31]. We consider τ lepton decays into muons, electrons and hadrons. The main background for decays into leptons $\tau \rightarrow \ell \nu \nu$ comes from ν_ℓ charged currents with charmed meson production. To reduce these backgrounds to a tolerable level, we first observe that a cut in the muon momentum reduces the background due to the decay of charged mesons at the level of 10^{-5} [29]; we then apply the *loose kinematical cuts* described in [29], which allow to retain a good efficiency for the signal. This means a global efficiency for τ signal events of $\varepsilon_\tau = 0.334$ (including the branching fractions to muons, electrons and hadronic channels) and a further reduction of the fractional background at the level of $5 \cdot 10^{-8}$.

For hadronic decays, the most important source of background comes from neutral current events. Also in this case, a fractional background at the level of 10^{-5} and a set of *loose kinematical cuts* reduce the fractional background at the level of $2 \cdot 10^{-7}$. The other backgrounds for leptonic τ decays quoted in [20] can be neglected.

If we fix the detector mass to 10 Kton (the minimum detector mass quoted for large LAr TPC project, see also [1]), we observe a general improvement on the fit quality with respect to the results obtained with an ECC*. This reflects in a better sensitivity to the octant of θ_{23} , as shown on the left panel of Fig. (4), to be compared with the right plot in Fig. (3).

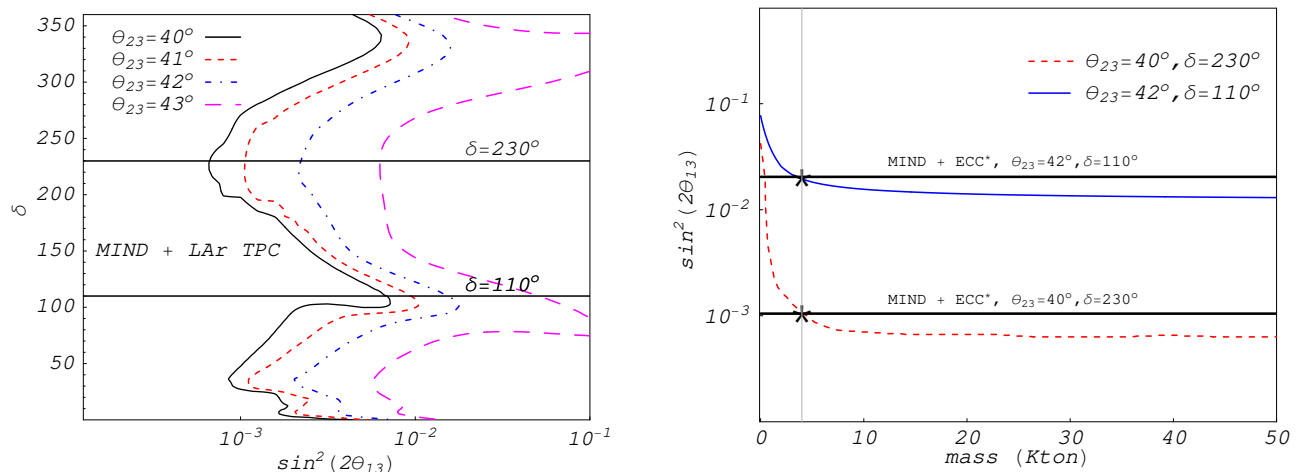


FIG. 4: *Left panel: Sensitivity to the θ_{23} octant at 3σ CL obtained combining the MIND and a 10 Kton LAr TPC detectors for different θ_{23} , from 40° to 43° . The horizontal lines highlight the values $\delta = 110^\circ$ and 230° . Right panel: 3σ CL sensitivity as a function of the LAr TPC detector mass. Continuum lines refer to $\theta_{23} = 42^\circ$ whereas long-dashed lines are computed for $\theta_{23} = 40^\circ$. The constant horizontal lines represent the sensitivities of the MIND+ECC* combination at two different points, $(\theta_{23}, \delta) = (40^\circ, 230^\circ)$ and $(42^\circ, 110^\circ)$. See text for details.*

The 10 Kton LAr TPC overwhelms the ECC* by about a factor of 2-3 in sensitivity, the main reasons being the larger detector mass. To verify this statement and compare both silver detectors, we proceed in the following way. From Fig. (3) and the left panel of Fig. (4), we can see that the sensitivity is maximal at $\delta \sim 230^\circ$ and minimal at $\delta \sim 110^\circ$, almost independently of θ_{23} . These values of δ are marked with horizontal lines in the left panel of Fig. (4). We then decide to performe the comparison using as a reference the sensitivity reach of the MIND+ECC* setup at the points $(\theta_{23}, \delta) = (40^\circ, 230^\circ)$ and $(42^\circ, 110^\circ)$, in which $\sin^2(2\theta_{13}) \sim 1.04 \cdot 10^{-3}$ and $\sin^2(2\theta_{13}) \sim 2.04 \cdot 10^{-2}$, respectively. These values are shown in the right panel of Fig. (4) as continuum horizontal lines. We can now compute

the sensitivities of the MIND+LAr TPC setup at the same (θ_{23}, δ) points as a function of the LAr TPC detector mass. The results are shown in the right panel of Fig. (4), in which the continuum line refers to the worse case $\theta_{23} = 42^\circ$ and the long-dashed line to the best case $\theta_{23} = 40^\circ$. The points in which these curves intersect the corresponding MIND+ECC* sensitivities define the values of the LAr TPC detector masses in which the sensitivities to the θ_{23} octant are the same for both silver detectors. It can be clearly seen that this happens for masses just around 4 Kton (as stressed by the stars and the gray vertical line in the left panel of Fig. (4)), implying a similar performance of both detectors when their masses are comparable. Notice that, as visible in the right panel of Fig. (4), an increase in the LAr TPC detector mass above 15-20 Kton does not improve the sensitivity to the θ_{23} octant since the systematic errors dominate over the statistical one and one cannot profit by the larger number of events.

V. DEVIATION FROM MAXIMAL MIXING

Having established the capability of the combination *golden+silver* to solve the octant ambiguity, we can now study the potential to exclude maximal θ_{23} . We define the sensitivity of the deviation from maximal mixing in the following way: for a given θ_{13} , we look for the largest value of θ_{23} for which the two-parameter 3σ contours do not touch $\theta_{23} = 45^\circ$. The results also depend on the assumed values of the atmospheric mass difference and the CP phase. While we retain Δm_{atm}^2 fixed to its best fit quoted in [25], we have analyzed the values $\delta = 110^\circ$ and $\delta = 230^\circ$, as in the previous section, and we have found not a large difference. For this reason, in Fig.5 we only quote the results obtained for $\delta = 230^\circ$ in the $[\sin^2(\theta_{23}) - \sin^2(2\theta_{13})]$ -plane. The $\sin^2(\theta_{23})$ variable is used since we have considered both octants of θ_{23} and we have found a behavior approximately symmetric of the sensitivity. As we can see, the MIND+LAr TPC combination is more sensitive to the deviation from maximal mixing compared to the MIND+ECC* result, an effect due to the larger detector mass considered. For $\sin^2(2\theta_{13}) \sim 10^{-3}$, there is fundamentally no possibility to tell a value for θ_{23} different from maximal mixing (notice that the smaller $\sin^2(\theta_{23})$ corresponds to $\theta_{23} \sim 40^\circ$). On the other hand, increasing θ_{13} one can explore deviations from $\sin^2(\theta_{23}) = 0.5$: at the larger value of $\sin^2(2\theta_{13})$, corresponding approximately to the CHOOZ bound $\theta_{13} \sim 13^\circ$ at 3σ CL [25, 32], deviation as small as 4% (6%) could be established combining the information from MIND and LAr TPC detectors (MIND and ECC*). For comparison, we mention that the neutrino factory setup with baseline $L = 7000$ Km described in [14] is able to see deviations from maximal mixing at 3σ for $\sin^2(\theta_{23})$ up to ~ 0.47 if $\sin^2(2\theta_{13}) = 7.6 \times 10^{-2}$ (and $\delta = 0$), a value which is in between the results shown in Fig.5.

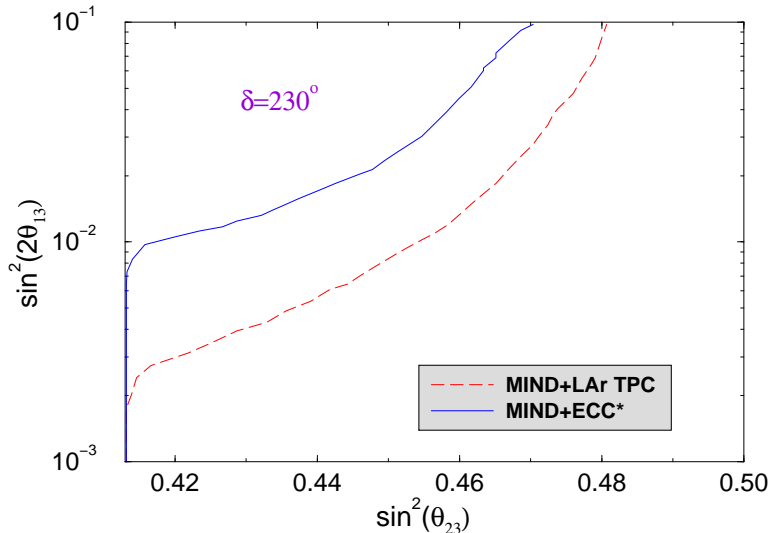


FIG. 5: 3σ sensitivity to maximal θ_{23} computed for $\delta = 230^\circ$. Solid line refers to the combination MIND+ECC* whereas the long-dashed line refers to MIND+LAr TPC setup.

VI. CONCLUSIONS

In this paper we have analyzed the potential of the combination of golden and silver transitions to solve the octant degeneracy problem, affecting the future measurement of θ_{13} and δ . Starting from the transition probabilities in

vacuum, we have shown that, in many cases, the octant clones are located in different points of the (θ_{13}, δ) -parameter space and that a promising synergy in solving this degeneracy exists. Our naive results are confirmed with detailed numerical simulations for a standard neutrino factory, in which a MIND detector has been used to look for the golden transition and an improved Emulsion Cloud Chamber detector and the Liquid Argon Time Projection Chamber have been employed to search for $\nu_e \rightarrow \nu_\tau$. As a general remark (almost independent on the silver detector), we observed that the octant degeneracy which mirrors the intrinsic clone gets solved in many of those cases in which the silver channel also eliminates the intrinsic degeneracy. However the octant clones which mirror the true points are much more difficult to eliminate, due to the very mild dependence on L/E and the silver channel, mainly due to the low statistics, is not enough to get rid of them. This ultimately lowers the sensitivity to the octant of θ_{23} . It is obvious that the problem of statistics can be circumvented (or at least relaxed) using an improved ECC detector (the ECC* option described in the paper, which couple a magnetic field to the standard ECC) or massive liquid argon detector with masses ranging from 10 to 100 Kton. A comparison between the physics potential of these two options strongly rely on the detector mass assumed to simulate the data. The very conservative (and probably more realistic) hypothesis of using a 5 Kton mass for the ECC detector and 10 Kton for the LAr TPC shows that the latter would be better in sensitivity by roughly a factor of three whereas, if a similar detector mass is used (around 4-5 Kton), the sensitivity reach of the two detectors is comparable, with $\sin^2(2\theta_{13}) \gtrsim 10^{-3}$ if $\theta_{23} = 40^\circ$.

We have also analyzed the capability of the two options to exclude maximal mixing at 3σ CL. We have found a better performance of the 10 Kton LAr TPC detector, being able to see deviations from $\theta_{23} = 45^\circ$ as small as 4% if θ_{13} is close to its upper limit. Using the ECC*, the possibility to exclude maximal mixing lowers to 6%.

We want to stress that these results have been obtained under reasonable assumptions for efficiency and backgrounds of the LAr TPC detector and that a simulation dedicated to the silver channel is still missing. Notice also that, contrary to what suggested in [13], we did not increase the mass of the ECC*, thus an improvement of its performance is a possibility that needed to be investigated further.

VII. ACKNOWLEDGMENT

D.M is strongly indebted to Andrea Donini for carefully reading the manuscript and for very useful suggestions. D.M. wants also thank M. Campanelli and A. Cervera for very useful discussions.

-
- [1] The ISS Physics Working Group, arXiv:0710.4947 [hep-ph].
 - [2] A. Cervera, A. Donini, M. B. Gavela, J. J. Gomez Cadenas, P. Hernandez, O. Mena and S. Rigolin, Nucl. Phys. B **579** (2000) 17 [Erratum-ibid. B **593** (2001) 731] [arXiv:hep-ph/0002108].
 - [3] A. Donini, D. Meloni and P. Migliozzi, Nucl. Phys. B **646** (2002) 321 [arXiv:hep-ph/0206034]; J. Phys. G **29** (2003) 1865 [arXiv:hep-ph/0209240].
 - [4] B. Pontecorvo, Sov. Phys. JETP **6** (1957) 429 [Zh. Eksp. Teor. Fiz. **33** (1957) 549]; Z. Maki, M. Nakagawa and S. Sakata, Prog. Theor. Phys. **28** (1962) 870; B. Pontecorvo, Sov. Phys. JETP **26** (1968) 984 [Zh. Eksp. Teor. Fiz. **53** (1967) 1717]; V. N. Gribov and B. Pontecorvo, Phys. Lett. B **28** (1969) 493.
 - [5] W-M Yao et al 2006 J. Phys. G: Nucl. Part. Phys. 33 1.
 - [6] J. Burguet-Castell, M. B. Gavela, J. J. Gomez-Cadenas, P. Hernandez and O. Mena, Nucl. Phys. B **608** (2001) 301 [arXiv:hep-ph/0103258].
 - [7] H. Minakata and H. Nunokawa, JHEP **0110** (2001) 001 [arXiv:hep-ph/0108085].
 - [8] G. L. Fogli and E. Lisi, Phys. Rev. D **54** (1996) 3667 [arXiv:hep-ph/9604415].
 - [9] V. Barger, D. Marfatia and K. Whisnant, Phys. Rev. D **65** (2002) 073023 [arXiv:hep-ph/0112119].
 - [10] G. Lin and Y. Umeda, arXiv:hep-ph/0612309.
 - [11] A. Donini, D. Meloni and S. Rigolin, JHEP **0406** (2004) 011 [arXiv:hep-ph/0312072].
 - [12] S. Geer, Phys. Rev. D **57** (1998) 6989 [Erratum-ibid. D **59** (1999) 039903] [arXiv:hep-ph/9712290]; A. De Rujula, M. B. Gavela and P. Hernandez, Nucl. Phys. B **547** (1999) 21 [arXiv:hep-ph/9811390].
 - [13] P. Huber, M. Lindner, M. Rolinec and W. Winter, Phys. Rev. D **74** (2006) 073003 [arXiv:hep-ph/0606119].
 - [14] A. Donini, E. Fernandez-Martinez, D. Meloni and S. Rigolin, Nucl. Phys. B **743** (2006) 41 [arXiv:hep-ph/0512038].
 - [15] S. Choubey and P. Roy, Phys. Rev. D **73** (2006) 013006 [arXiv:hep-ph/0509197].
 - [16] K. Hiraide, H. Minakata, T. Nakaya, H. Nunokawa, H. Sugiyama, W. J. C. Teves and R. Zukanovich Funchal, Phys. Rev. D **73**, 093008 (2006) [arXiv:hep-ph/0601258].
 - [17] T. Kajita, H. Minakata, S. Nakayama and H. Nunokawa, Phys. Rev. D **75** (2007) 013006 [arXiv:hep-ph/0609286].
 - [18] K. Hagiwara and N. Okamura, arXiv:hep-ph/0611058.
 - [19] J. Burguet-Castell, M. B. Gavela, J. J. Gomez-Cadenas, P. Hernandez and O. Mena, Nucl. Phys. B **646** (2002) 301 [arXiv:hep-ph/0207080].
 - [20] D. Autiero *et al.*, Eur. Phys. J. C **33**, 243 (2004) [arXiv:hep-ph/0305185].

- [21] ISS report, accelerator working group.
- [22] A. Cervera, F. Dydak and J. Gomez Cadenas, Nucl. Instrum. Meth. A **451** (2000) 123.
- [23] A. Cervera, private communication.
- [24] A. Cervera, *MIND, a Magnetized Iron Neutrino Detector*, talk given at "Golden07", June 27-30 2007, Valencia (Spain);
A. Cervera, *MIND performance and prototyping*, talk given at "NuFact07", August 6-11 2007, Okayama (Japan).
- [25] M. C. Gonzalez-Garcia and M. Maltoni, arXiv:0704.1800 [hep-ph].
- [26] P. Huber, M. Lindner and W. Winter, Comput. Phys. Commun. **167** (2005) 195 [arXiv:hep-ph/0407333]; P. Huber, J. Kopp, M. Lindner, M. Rolinec and W. Winter, arXiv:hep-ph/0701187.
- [27] G. de Lellis, *Magnetized Emulsion Cloud Chambers detectors*, talk given at "Golden07", 27-30 June 2007, Valencia (Spain).
- [28] P. Aprili *et al.* [ICARUS Collaboration], "The ICARUS experiment: A second-generation proton decay experiment and neutrino observatory at the Gran Sasso laboratory. Cloning of T600 modules to reach the design sensitive mass. (Addendum)," CERN-SPSC-P-323.
- [29] A. Bueno, M. Campanelli and A. Rubbia, Nucl. Phys. B **589** (2000) 577 [arXiv:hep-ph/0005007].
- [30] A. Rubbia, arXiv:hep-ph/0402110;
A. Rubbia, *GLACIER, a magnetised liquid argon TPC*, talk given at "Golden07", 27-30 June 2007, Valencia (Spain).
- [31] A. Campanelli, private communication.
- [32] M. Apollonio *et al.* [CHOOZ Collaboration], Eur. Phys. J. C **27**, 331 (2003) [arXiv:hep-ex/0301017].